In Situ Observations of Cometary Nuclei

H. U. Keller
Max-Planck-Institut für Aeronomie

D. Britt
University of Central Florida

B. J. Buratti
Jet Propulsion Laboratory

N. Thomas
Max-Planck-Institut für Aeronomie
(now at University of Bern)

It is only through close spacecraft encounters that cometary nuclei can be resolved and their properties determined with complete confidence. At the time of writing, only two nuclei (those of Comets 1P/Halley and 19P/Borrelly) have been observed, both by rapid flyby missions. The camera systems onboard these missions have revealed single, solid, dark, lumpy, and elongated nuclei. The infrared systems gave surface temperatures well above the free sublimation temperature of water ice and close to blackbody temperatures. The observed nuclei were much more similar than they were different. In both cases, significant topography was evident, possibly reflecting the objects' sublimation histories. Dust emission was restricted to active regions and jets in the inner comae were prevalent. Active regions may have been slightly brighter than inert areas but the reflectance was still very low. No activity from the nightside was found. In this chapter, the observations are presented and comparisons are made between Comets Halley and Borrelly. A paradigm for the structure of cometary nuclei is also described that implies that the nonvolatile component defines the characteristics of nuclei and that high porosity, large-scale inhomogeneity, and moderate tensile strength are common features.

1. INTRODUCTION

The nuclei of most comets are too small to be resolved by Earth-based telescopes. Even on the rare occasions when a large, possibly resolvable, long-period comet, such as Comet Hale-Bopp (C/1995 O1), enters the inner solar system, the nucleus is obscured from view by the dust coma. Hence, the only means of studying the details of a cometary nucleus is by using interplanetary space probes.

Spacecraft passages to within 10,000 km allow many different techniques to diagnose the properties of the nucleus. The most obvious is high-resolution imaging. However, there are several other remote sensing techniques that could give important information. Only visible and infrared spectroscopy have been used, giving estimates of the surface temperatures of both Comet 1P/Halley and Comet 19P/Borrelly. Indirect measurements through analysis of the volatile (gas) and nonvolatile (dust) components *in situ*, for example, are also vital to our understanding of cometary nuclei since they give information on the composition and structure of the nucleus. Ion mass spectrometers have been particularly useful in this respect for our current understanding.

It is important to emphasize that prior to the spacecraft encounters with Comet 1P/Halley in 1986, the existence of a nucleus was merely inferred from coarse observations. While the idea that a single, small, solid body was at the center of a comet's activity (*Whipple,* 1950) was widely accepted by the scientific community, it was only with the arrival of the Russian *Vega 1* and *2* and European Space Agency's *Giotto* spacecraft at Comet Halley in 1986 that this could be confirmed and other concepts [e.g., the "sandbank" model of *Lyttleton* (1953)] could finally be rejected. It was to be 15 years before another image of a cometary nucleus would be acquired, when NASA's *Deep Space 1* (*DS1*), a technology development mission, successfully imaged the nucleus of Comet 19P/Borrelly in September 2001. Remarkably, the two nuclei observed by these missions were extremely similar.

Comet Halley is the most prominent member of comets on highly inclined (162.24°) and eccentric (0.967) orbits, which are thought to have been members of the Oort cloud. Its period was 76.0 yr and its perihelion distance 0.587 AU. It is one of the most active short-period comets. Therefore, its appearance during the space age triggered the launch of

TABLE 1. Cometary flybys.

Spacecraft	Closest Approach Distance (km)	Date and Time of Closest Approach	Flyby Velocity (km s^{-1})	Heliocentric Distance (AU)	Phase Angle of Approach (degrees)	Best Pixel Scale Obtained (m/pixel)	Comment on Imaging Systems and Data
Vega 1	8890	06.03.1986 07:20:06	79.2	0.792	134		Out of focus (FWHM = 10 pixels)
Vega 2	8030	09.03.1986 07:20:00	76.8	0.834	121		Saturated on nucleus
Giotto	596	14.03.1986 00:03:02	68.4	0.89	107.2	38	Little three-dimensional information because of reset 9 s before closest approach
Deep Space 1	2171	22.09.2001	16.5	1.36	88.0	47	Some stereo information, minimum phase angle 52°, no color

the "Halley Armada," comprising five spacecraft that encountered the comet in spring 1986. The Japanese probes, Suisei and Sakegaki (*Hirao and Itoh,* 1987), did not penetrate the comet's inner coma and did not carry experiments for studying the nucleus. The *Vega 1* and *2* spacecraft made encounters on March 6 and 9, 1986, respectively (Table 1). Just after midnight on March 14, 1986, the *Giotto* spacecraft made its closest approach (596 km). The *Vega* and *Giotto* spacecraft all carried sophisticated remote sensing experiments for determination of the properties of the nucleus, and we discuss those results in turn in section 2. In section 3, we discuss the results on the nucleus of Comet 10P/Borrelly obtained from the *DS1* mission.

2. COMET HALLEY'S NUCLEUS

2.1. *Vega* Observations

The *Vega* cameras imaged the nucleus throughout their encounters with Comet Halley. However, both imaging systems experienced severe problems. The *Vega 1* television system (TVS) system was out of focus. The point-spread function (PSF) of the instrument was subsequently found to be at least 10 pixels full-width half-maximum (FWHM), caused by a displacement of the detector with respect to the focal plane of about 0.5 mm (*Abergel and Bertaux,* 1995). This effect degraded the effective resolution from around 150 m (at closest approach) to 1.5 km at best and made the images appear extremely fuzzy. While the nucleus was resolved and observed over a range of phase angles, a huge amount of work (e.g., *Merényi et al.,* 1990) had to be invested to correct the images for the degraded PSF and to derive the basic shape of the nucleus. This has proven to be important since the orientation of Comet Halley's nucleus at the time of the *Vega 1* encounter provides a strict constraint on models of the rotational state of the comet (*Belton,* 1990) (see below).

The *Vega 2* TVS also experienced problems. The images are saturated on the nucleus and the data of the coma that were returned are limited in dynamic range to effectively only 5 bits (32 gray levels) digital resolution. While these data are of little interest for direct studies of the nucleus surface, they do provide some information on the near-nucleus jet structures of Comet Halley (Fig. 1). In particular, the data indicate a sunward "fan" of dust emission (*Larson*

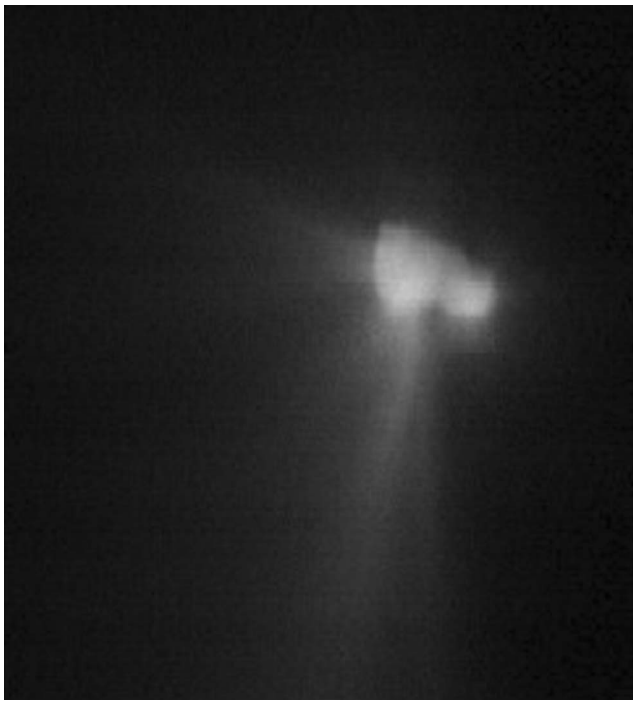

Fig. 1. The *Vega 2* image (#1690) from the *Vega* atlas of Comet 1P/Halley (*Szegö et al.,* 1995) is cleaned and geometrically corrected. It shows the nucleus and its vicinity from a distance of 8030 km (near closest approach) at a phase angle of 28° on March 9, 1986.

et al., 1987) that may have originated from a quasi-linear "crack" in the surface (see also *Szegö et al.,* 1995). The data therefore suggest that activity is restricted to "active regions" (confirmed by *Giotto* images). The lack of structure in the comae of some short-period comets [e.g., Comet 4P/Faye (*Lamy et al.,* 1996)] may indicate a more homogeneously active surface may be appropriate for some nuclei, but *Vega*, *Giotto*, and *DS1* images clearly show that this is not the case for Comets Halley and Borrelly.

Further support for limited areas of activity comes from the *Vega* IKS experiment, which determined the surface temperature of Comet Halley's nucleus. Temperatures in excess of 350 K were recorded (*Emerich et al.,* 1987a,b). A surface undergoing free sublimation of water ice (at 1 AU heliocentric distance) can only reach an equilibrium temperature of about 220 K even for low albedo values. The IKS measurement indicates that significant parts of Comet Halley's surface were inactive. Care in the interpretation is necessary, however, because micrometer-sized dust particles from the surface rise in temperature rapidly once ejected. If the optical depth, τ, of these particles approaches 1, the effect is to mask the thermal emission from the (possibly) lower temperature surface.

Indeed, the first impressions of the *Vega* TVS data suggested $\tau \approx 1$ (based, to some extent, on the fuzziness of the pictures now attributed to defocusing). This temperature measurement has not been rediscussed subsequently, but support for high surface temperatures came from the *DS1* flyby (*Soderblom et al.,* 2002) where optical depth was not a problem because the activity of Comet Borrelly was more than one order of magnitude lower than that of Comet Halley (at the encounters). These high temperatures confirm that activity is restricted and most of the surface of both comets is inert.

After the *Vega* encounters the size and shape of the nucleus of Comet Halley was not obvious. It was not even clear that there was only a single nucleus. False color images artificially cropped at certain isophote levels [e.g., cover images of *Sagdeev* (1988) and *Szegö et al.* (1995)] are strongly misleading if interpreted as showing the nucleus. It took the observations of the subsequent *Giotto* flyby to provide the basic information for the interpretation of the *Vega* images.

2.2. *Giotto* Observations

2.2.1. Imaging by the Halley Multicolour Camera. More than 2000 images of Comet Halley's coma and nucleus were acquired by the Halley Multicolour Camera (HMC) onboard the *Giotto* spacecraft. A detailed description of the observations and results is given by *Keller et al.* (1995). During approach, the phase angle was 107° and changed only slightly up to the last good image taken from a distance of 2000 km with a resolution of 45 m/pixel. The *Giotto* spacecraft was then hit by large dust particles and lost contact to ground. A representative sample of images is shown in Fig. 2.

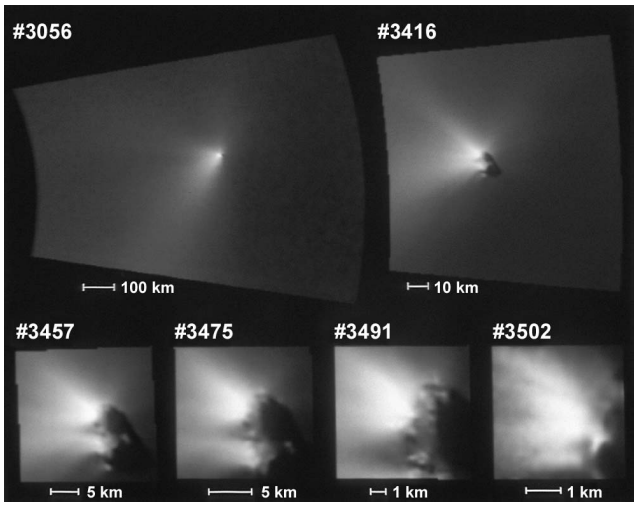

Fig. 2. Six examples of HMC images of P/Halley in original frame sizes. Image #3056 was taken 1814 s (distance to nucleus 124,000 km) and image #3502 was taken 31 s (2200 km) before closest approach.

2.2.2. Bulk properties of the nucleus. In the HMC images only ~25% of the surface area accessible to the camera is illuminated by the Sun, owing to the large phase angle. Fortuitously, the outline of the dark limb is visible against the illuminated dust in the background. This unique circumstance provided a good enough constraint that the fuzzy *Vega* images taken from different solar and rotational phase angles could be interpreted and the bulk properties (volume) of the nucleus could be determined. The maximum length of the nucleus from *Vega* images was 15.3 km. A comparison with the length seen by HMC (14.2 ± 0.3 km) requires the long axis of the nucleus to be 22° above or below the image plane. A major effort of the *Vega* team went into defining the orientation and illuminated outline of the nucleus for both of the flybys (*Merényi et al.,* 1990; *Stooke and Abergel,* 1991). Additional constraints come from the period(s) of the cometary brightness fluctuations derived from Earth-based observations (see also section 2.2.5). Various solutions of the rotation axis and period(s) were suggested [more elaborate interpretations come from *Belton et al.* (1991) and *Szegö et al.* (1995)], but none satisfies all the constraints. The solution by *Belton et al.* (1991) needs the "thick and the thin" ends of the nucleus on the *Vega 1* images interchanged from the orientation derived by the *Vega* team. In addition, the distribution of active areas on the nucleus surface does not satisfy the constraints derived from HMC images. A best fit triaxial ellipsoid with 7.2, 7.22, and 15.3 km for the axes was derived by *Merényi et al.* (1990) with an estimated error of 0.5 km in each figure. Taking into account the deviations from this ellipsoid (with a volume of 420 km^3) led to an estimated volume of 365 km^3 and an overall surface of 294 km^2 for Comet Halley's nucleus. Combining this volume with a mass estimate of $1–3 \times 10^{14}$ kg (*Rickman,* 1989) determined from nongravitational forces yields a density of the nucleus of 550 ± 250 kg m^{-3}. Other estimates of the

density yield a wider range, not excluding the "intuitive" value of 1000 kg m^{-3} (*Sagdeev et al.,* 1988; *Peale,* 1989).

A surprisingly (at that time) low geometric albedo of $0.04^{+0.02}_{-0.01}$ of the nucleus was derived from *Vega* images (*Sagdeev et al.,* 1986) assuming a Moon-like phase function. Similar values are found for other comets from groundbased visible and IR observations (*Keller and Jorda,* 2002; *Lamy et al.,* 2004). Comets are among the darkest objects of the solar system. This albedo of 0.04, measured directly for the first time, has been widely used as a canonical value to determine sizes from photometric observations. The reflectivity of the illuminated surface derived from HMC images for a phase angle of 107° was found to be less than 0.6% (*Keller et al.,* 1986). Fitting the observed reflectivity (I/F) across the illuminated surface seen in the HMC images confirmed the Moon-like phase function and yielded a reflectivity at zero phase angle between 0.05 and 0.08, in reasonable agreement with estimates of the peak reflectivity (*Keller et al.,* 1995; *Thomas and Keller,* 1989).

The color of the nucleus was found to be slightly reddish with a gradient of 6 (±3)% per 100 nm between 440 nm and 810 nm (*Thomas and Keller,* 1989), similar to P-type asteroids. The variation of the reflectivity over the visible surface was moderate (*Keller,* 1989), somewhat in contrast to the results of the more detailed observations of the nucleus of Comet Borrelly (see section 3.1). No "icy" patches could be seen, either on HMC or on *Vega* images. Active areas may possibly be slightly brighter than their surroundings, but the increased dust density could confuse the issue. Pure water ice on the surface can be ruled out. However, small contaminations of the ice with carbon suffice to reduce the reflectivity to the observed low value.

2.2.3. Topography and morphology. Two spheres, a larger one on the south end (Fig. 3), connected to each other creating a "waist" would be a higher mode approximation than the ellipsoid. The near 2 : 1 elongation of the nucleus is rather typical for cometary nuclei (*Keller and Jorda,* 2002; *Lamy et al.,* 2004). Prominent large-scale features are

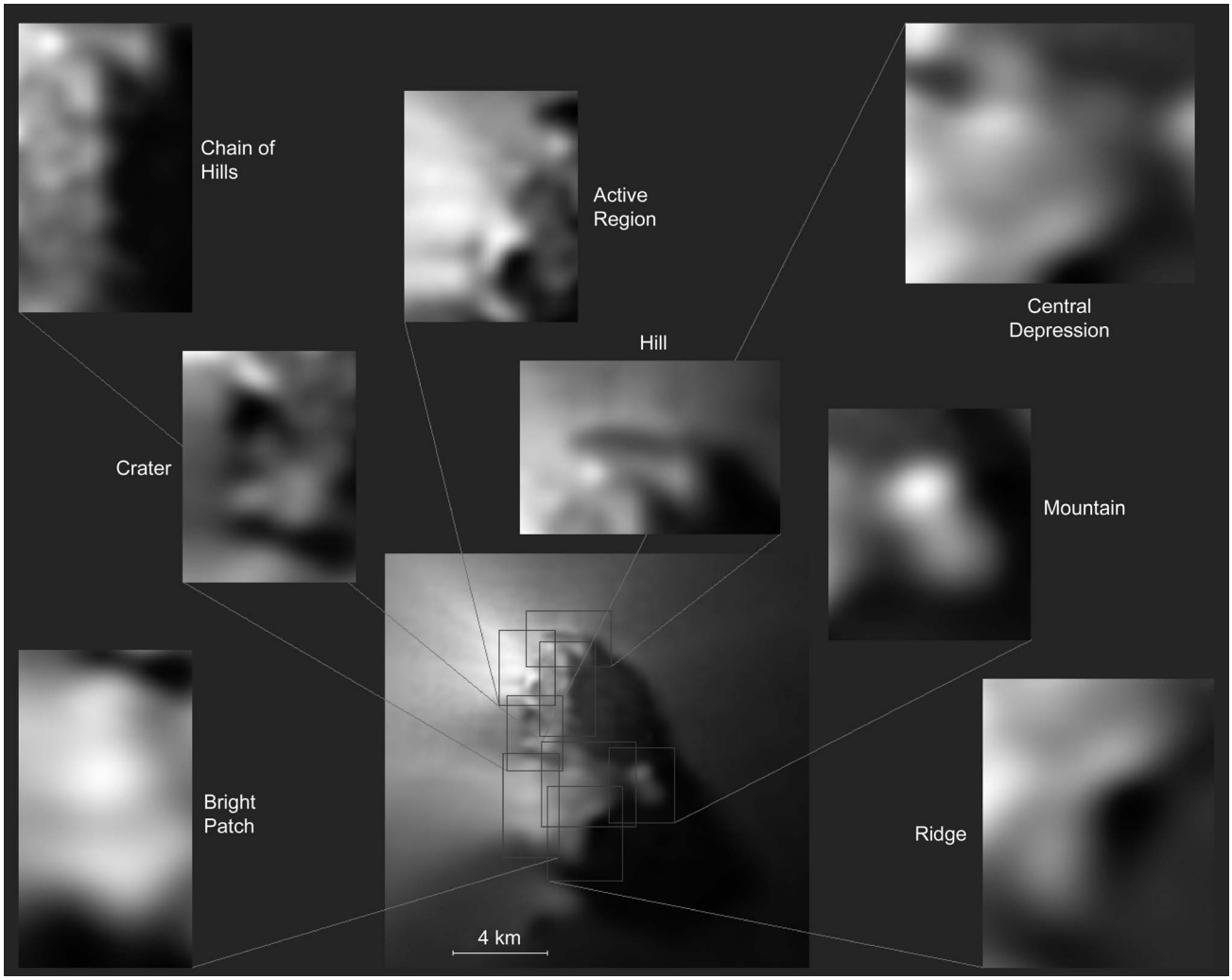

Fig. 3. Features on the surface of the nucleus of Comet 1P/Halley. Sections of the composite image (center bottom) are extracted and expanded by a factor of 3 to show, in detail, notable features on the nucleus mentioned in the text. Nonlinear enhancement has been applied to provide improved contrast. From *Keller et al.* (1988).

the northeastern limb that follows a straight line and terminates in an almost rectangular corner (*duck tail*) that protrudes by $\Delta R/R = 0.3$ above the radius of the best-fit ellipsoid. The terminator on the south (morning) side of the *central depression* paralleled by a bright band (*ridge*) indicates a large-scale feature such as a terrace. The central depression tapers toward the *mountain*. Its illuminated tip lies about 900 m above the best-fit ellipsoid. For more details, see *Keller et al.* (1995).

The roughness of the nucleus is visible down to the resolution limit of the HMC observations (45 m/pixel). The *chain of hills* are an example for the typical scalelength of 0.5–1 km; others are the structures inside the *crater*. It covers a projected area of 12 km^2 and its depth was estimated to be only 200 m (*Schwarz et al.,* 1986). Most topographic features may be shallow because of the large solar zenith angle (long shadows) during the HMC observations. The strongly irregular shape, the protrusions, the topographic features, the high porosity and low gravity of the nucleus, and the predominance of nonvolatile material all suggest that the surface morphology is characterized by roughness down to small scales (*Kührt et al.,* 1997).

2.2.4. Activity.

2.2.4.1. Overall activity: Activity characterized by dust jets or cones can be directly observed at the illuminated area just below the northern tip of the nucleus around the subsolar point and in direction roughly toward the Sun. In this region the maximum brightness of the images is observed just above the limb. The strongest jet, however, does not originate from this location. At radial distances from the surface lager than the radius of the nucleus, the maximum of the dust column density shifts to an azimuth about 40° south of the projected comet-Sun direction, the direction of the strongest dust jet. Dust emission into this direction is about three times stronger than the subsolar jet and dominates the overall shape of the dust coma (compare the images of Fig. 2). This strong jet originates from the illuminated hemisphere turned away from the observer (*Thomas and Keller,* 1988). A third rather weak jet is directed (in projection) about 90° off the comet-Sun direction toward the north. The overall shape of the dust isophotes can be well modeled by the superposition of these three jets with a cone width of ~40° (FWHM). *Belton et al.* (1991) identified five jets from groundbased, *Vega*, and *Giotto* images. The position of their main jet, however, is not in agreement with the HMC observations.

2.2.4.2. Structures and filaments and topography: The extent of the visible active area covers about 3 km along the bright limb. Here the highest-resolution images taken show structures on the surface and in the dust jet above it. Narrow filamentary structures can be discerned starting at the surface with footprints about 500 m in diameter. Some of these filaments can be followed out to more than 100 km (*Thomas and Keller,* 1987a,b). Overall, more than 15 narrow jets and filaments, some strongly collimated with opening angles of a few degrees, were revealed by image processing (Fig. 4). Some of the filament directions cross each other, obviously due to the influence of topography (*Thomas et al.,* 1988; *Huebner et al.,* 1988). A few filaments point away from the Sun, emerging behind the dark limb. They probably originate from the small insolated sliver of the nucleus apparently pointing, in projection, in the antisolar direction. No indications of activity on the nightside of the nucleus were found.

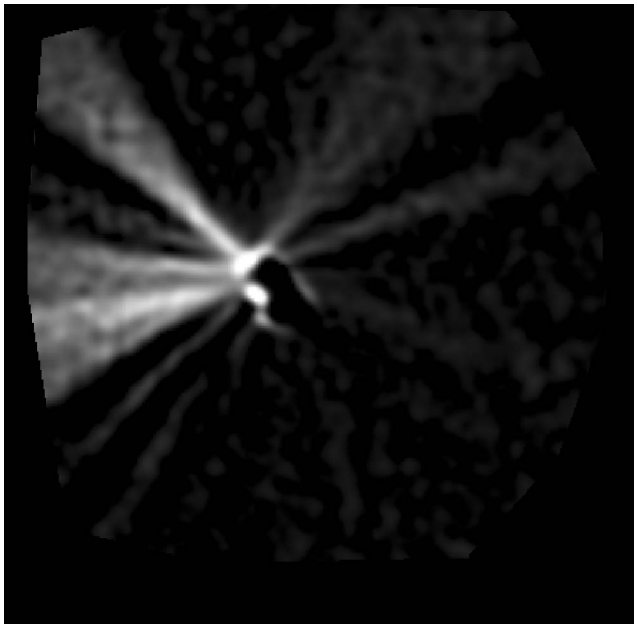

Fig. 4. The directions of "filaments" seen in the dust emission. The filaments are small inhomogeneities (500 m in diameter at their source). This fine structure in the emission would have been far too faint to be seen by simultaneous groundbased observers. The filaments appear to criss-cross each other.

The interaction of jet features is also evidenced by the curved dark area in the dust just in front of the lower end of the *bright patch*. A three-dimensional gas dynamics calculation confirms this interaction, mainly caused by the concavity (Fig. 3) at the waist (*Crifo and Rodionov,* 1999). In a series of papers, *Crifo et al.* (2002) and *Rodionov et al.* (2002) have modeled the observations based on the assumption of a uniformly active homogenous nuclear surface rather than on limited active areas within a predominantly inert surface. They assume that the dust production is proportional to the insolation. This leads to a strong concentration of the dust production (and density) toward the Sun-comet line and in the sunward hemisphere. The ratio of the integrated dust of the sunward to that of the antisunward hemisphere would then be about an order of magnitude larger than observed (section 3.2) (see *Keller et al.,* 1995). While Comet Halley was active enough that the hypothesis of a homogenous surface activity could be justified and tested, the jets observed during the flyby of Comet Borrelly (see section 3.3) obviously cannot be explained by a homogenously active surface.

The limited width (FWHM $\approx 40°$) of the major jets suggests that they do not originate from flat or convex active

areas on an otherwise inert surface. Shallow indentations, however, like the *crater* or larger concave topography (like the *bright patch*) suffice to collimate the dust (*Keller et al.,* 1992). A crude axisymmetric gas-dynamics model that describes the acceleration of dust particles (typically 10 μm) from the surface (*Knollenberg,* 1994) was used to simulate these jets. The narrow fine filaments with opening angles of a few degrees cannot be explained by cavities that would be too deep for the Sun to reach their bottoms. Rather than by an enhancement of activity, the filaments can be formed by reduction of activity in the center of an active area simulating strong (axisymmetric) interactions of shock fronts (*Keller et al.,* 1995).

2.2.5. Nucleus rotation. Shortly after the encounters with Comet Halley, the rotation period of the nucleus was derived by comparing the various images during the three flybys. In a first-order approach, a stable rotation around the axis of maximum inertia (perpendicular to the long axis) was assumed (*Wilhelm,* 1987; *Sagdeev et al.,* 1989). Fits were found for a period slightly above 50 h (2.2 d). Groundbased observations of the coma brightness variations yielded a period of about 7 d, but dynamical features (jets, shells) were in agreement with the 2.2-d periodicity. It is now widely assumed that the spin state of Comet Halley is excited, i.e., that the rotation is not in its energetic minimum and includes nutation (*Sagdeev et al.,* 1989; *Samarasinha and A'Hearn,* 1991; *Belton et al.,* 1991). There is no common understanding of the details (*Keller and Jorda,* 2002). Three flybys and a long series of groundbased observations were not sufficient to pin down the rotational parameters.

3. COMET BORRELLY'S NUCLEUS

The next spacecraft close encounter with a comet occurred on September 22, 2001 when the *DS1* spacecraft flew by the Comet 19P/Borrelly. The *DS1* mission was primarily an engineering test of a solar-electric ion-propulsion system, but part of the mission goals were to test spacecraft instruments and software with close flybys of small bodies. The primary data for this paper comes from imagery taken by the Miniature Integrated Camera and Spectrometer (MICAS) instrument, which included a 1024 × 1024 frame-transfer CCD. The mission plan was to fly by Comet Borrelly with a miss distance of approximately 2000 km on the sunward side at a relative speed of 16.5 km s^{-1} (*Soderblom et al.,* 2002). Because MICAS was in a fixed orientation on the spacecraft, the whole spacecraft was rotated to keep Comet Borrelly in the field of view.

During the 90 minutes before closest approach, 52 visible wavelength images were taken with MICAS at solar phase angles between 88° and 52°. Shown in Fig. 5 is the highest-resolution image, taken at 3556 km from the comet, with a resolution of 47 m/pixel. Because Comet Borrelly has a long rotation period of 25 ± 0.5 h, *DS1* saw essentially only the illuminated part of one hemisphere of the comet. The full shape and volume of the nucleus could not be revealed. Matching images taken between solar phase angles of about 60° and 52° provides stereo pairs and reveals coarse topographic information. Based on this digital terrain model, morphological and photometric information of the surfaces of various terrains can be derived. These more detailed analyses and interpretations have recently been published in a special volume of *Icarus* devoted mainly to the *DS1* flyby of Comet Borrelly. Here we provide a summary of those results.

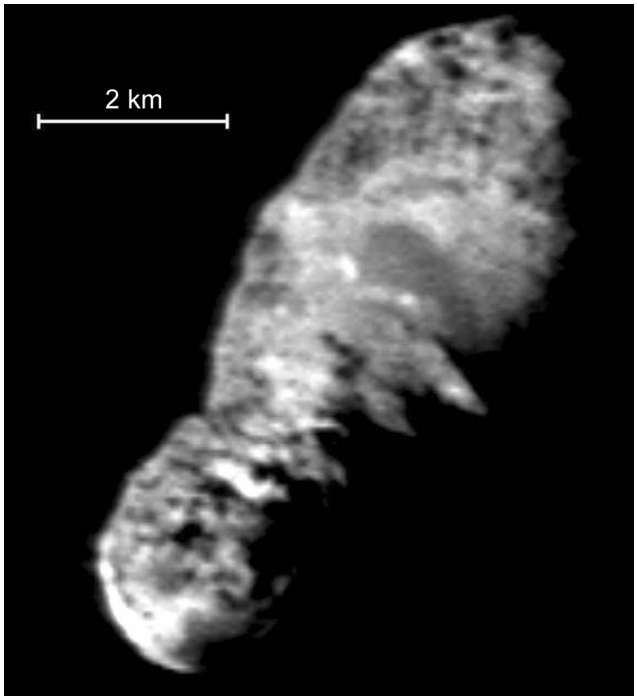

Fig. 5. The highest-resolution image of the Comet 19/P Borrelly. This image was taken at 3556 km from the comet and has a scale of 47 m/pixel.

Comet 19P/Borrelly is a Jupiter-family comet with an orbital period of 6.86 yr, a semimajor axis of 3.61 AU, an inclination of 30.24°, and a perihelion distance of 1.359 AU. The flyby occurred eight days after perihelion while the comet was crossing the ecliptic. *DS1* imagery showed an 8.0 ± 0.1 km × 3.15 ± 0.08 km object shaped like a left footprint with a heel at the bottom of Fig. 5 and the sole toward the top. The rotation axis derived from Earth-based observations corresponds to the short axis exiting near the central mesa (see section 3.2). The pole obliquity and orbital longitude are 102.7° ± 0.5° and 146° ± 1°, corresponding to RA = 214.01° and DEC = –5.07° (*Schleicher et al.,* 2003). The pole is pointed sunward, with a subsolar latitude of ~60° during the encounter (*Soderblom et al.,* 2002). Comet Borrelly has an average disk integrated geometric albedo of 0.029 ± 0.006 (*Buratti et al.,* 2004), even slightly lower than the value measured for Comet Halley (see section 2.2.2). The albedo values of Comet Halley and Comet Borrelly are comparable to those of other dark bodies in the solar system, including the low-albedo regions of Iapetus (*Buratti and Mosher,* 1995), the uranian rings (*Ockert et al.,* 1987), and the lowest-albedo C-type asteroids (*Tedesco et al.,* 1989), including several in comet-like orbits (*Fernández et al.,* 2001).

3.1. Disk-Integrated Photometry

The *DS1* encounter with Comet Borrelly enabled the first photometric modeling of a cometary nucleus. Physical attributes of the surface of the nucleus, including the compaction state of the optically active portion of the regolith and the macroscopic roughness, can be derived by fitting photometric models to the observed brightness as a function of viewing geometry. The nucleus must be observed over a range of solar phase angles to perform this type of analysis.

Figure 6 shows a disk-integrated solar phase curve of Comet Borrelly created from Earth-based observations (*Lamy et al.,* 1998; *Rauer et al.,* 1999) and spacecraft measurements, along with a disk-integrated fit to Hapke's photometric model (*Hapke,* 1981, 1984, 1986). The derived single scattering albedo w = 0.020 and the asymmetry of the phase function g = –0.45 led to an opposition surge amplitude of $B_0 = 1.0$ and low compaction indicated by the parameter h = 0.0084. The mean slope angle of 20 relates to surface roughness on scales ranging from clumps of particles to mountains.

Comet Borrelly's nucleus has surface physical properties similar to those of C-type asteroids (*Helfenstein and Veverka,* 1989). The single-scattering albedo is lower than measured for any other body. The phase integral derived from the data in Fig. 6 is 0.27 ± 0.01, to yield a Bond albedo of 0.009 ± 0.02, again the lowest of any object in the solar system so far measured. These values, however, depend critically on the few Earth-based measurements.

The extremely low albedo values require high microporosity of the surface that traps the light very efficiently. Appropriate modeling will have to show whether these values can be reached with realistic physical properties.

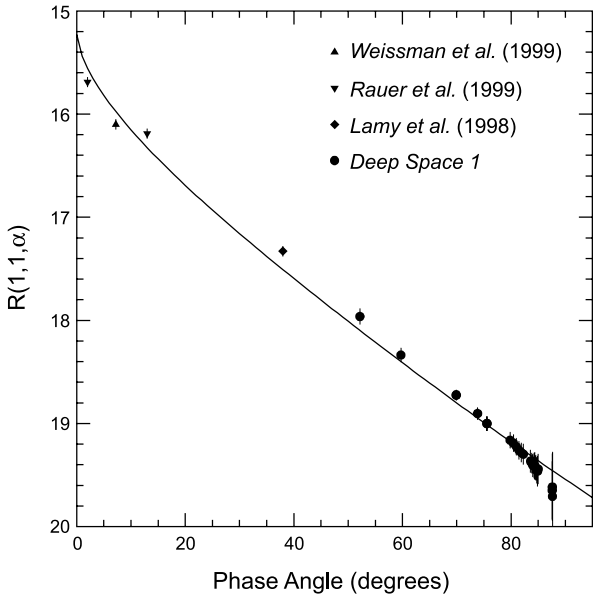

Fig. 6. The disk-integrated solar phase curve of Borrelly created from groundbased, spacebased (HST), and spacecraft (*DS1*) observations.

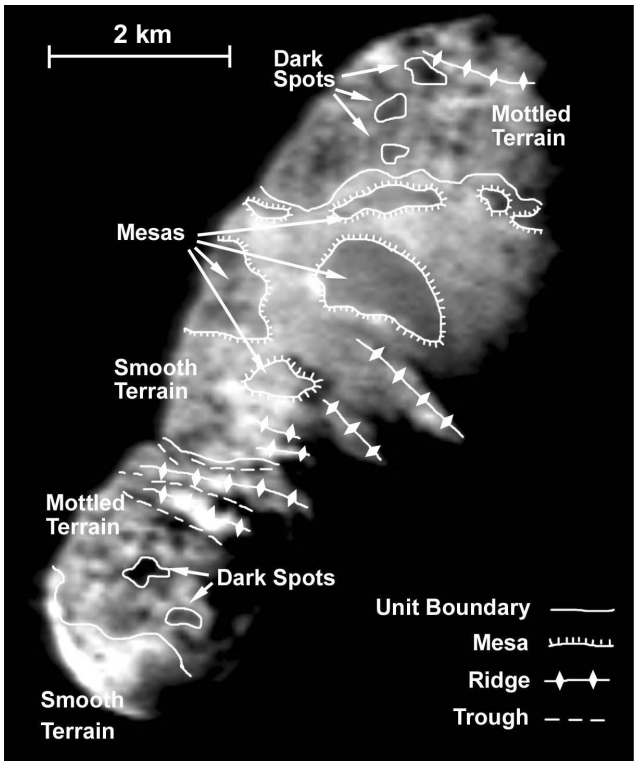

Fig. 7. Unit and feature map of Borrelly based on analysis of the MICAS imagery, including stereo pairs.

3.2. Surface Morphology

Comet Borrelly has a complex surface with a range of morphological features. Interpretations of these features based on analysis of the MICAS imagery, including stereo pairs, are shown in Fig. 7. Four major morphological units can be discerned — dark spots, mottled terrain, mesas, and bright terrain — and two surface features — ridges and fractures. One of the most interesting (but expected) results is the absence of impact craters, commonly associated with small bodies. The upper limit for their diameters is 200 m (*Soderblom et al.,* 2002). While there are a number quasi-circular depressions visible, they are most abundant in the mottled terrain and have roughly similar diameters and sometimes regular spacing (cf. the chain of hills on the surface of Comet Halley). Our analysis suggests that they may be sublimation features. Using a simple shape model, a Lommel-Seeliger photometric function, and the phase curve illustrated in Fig. 6, a map of normal reflectances (*Buratti et al.,* 2004) illustrates variegations up to a factor of almost four in albedo (from 0.012 to 0.045) that are correlated with geologic terrains and features. For low-albedo objects such as Comet Borrelly, normal reflectance and geometric albedo are equivalent.

Dark spots: These are the darkest areas on the comet, with a geometric albedo around 0.015. Photometric profiles of the dark spots confirm that they are not shadowed and have photometric properties similar to the mottled terrain (*Nelson et al.,* 2004; *Buratti et al.,* 2004). Dark spots appear to overlie the mottled terrain and hence are the strati-

graphically highest unit on Comet Borrelly. They probably represent the oldest surface lags.

Mottled terrain: The mottled terrain is stratigraphically below the dark spots and consists of areas rough at pixel resolution with depressions, troughs, hills, and ridges. The terrain is dominated by a mixture of quasicircular depressions and low hills. The quasi-circular depressions are about 200–300 m in diameter and are most common on the heel portion of the comet. Low hills tend to be roughly aligned along the long axis of the comet and spaced approximately 300–400 m apart (cf. the chain of hills on Comet Halley; see section 2.2.3). The morphology and albedo variations suggest that the mottled terrain represents older surface lag deposits that have been subjected to extensive sublimation erosion leading to terrain softening and collapse (*Britt et al.,* 2004).

Mesas: Mesas consist of several areas of steep, bright-appearing slopes surrounding darker, flat tops. These features are primarily in the central portion of the comet and appear, along with the smooth terrain, to be associated with some of the active jets. Mesa formation is probably driven, like terrestrial mesas, by erosion (sublimation) on the steep slopes. The mesa slopes are probably one of the most freshly exposed areas on the comet and may be a source of significant gas/dust loss.

Smooth terrain: Photometric analysis suggests that this unit is slightly rougher than average at subpixel scales with geometric albedos of typically 0.032 and in some spots as high as 0.045 (*Buratti et al.,* 2004). The fine pattern of albedo variegations may indicate areas of differential activity and/or surface age as part of the resurfacing processes from dust ejection.

Ridges and fractures: Digital terrain models indicate that the area of the heel is canted about 15° relative to the sole (*Soderblom et al.,* 2002; *Oberst et al.,* 2004). Most of the ridges and fractures are associated with the boundary of this canted area. These ridges of 1–2 km in visible length are oriented normal to the long axis of the comet and could indicate compressional shortening (*Britt et al.,* 2004). If this interpretation is correct, the features require some tensile strength of the nucleus.

3.3. Jets and Active Areas

DS1 observed dust and gas activity including collimated jets and fans (*Soderblom et al.,* 2002). The largest central jet, called the α jet, is a dusty beam a few kilometers wide at the comet (cf. active areas of Comet Halley; see section 2.2.4.1), extending out to at least 100 km and canted 30° from the comet-Sun line (Fig. 8). This feature appears to emanate from the broad central area of the comet, which includes the mesas and the smooth terrain. There are several smaller parallel jets, called the β jets, which are about 200–400 m at the base [cf. filaments of Comet Halley (section 2.2.4.2)], about 4–6 km in length, and canted about 15° from the direction of the α jet. The fan feature is diffuse dust apparently emanating from the smooth terrain unit at the end of Comet Borrelly's heel and oriented roughly along the Sun-comet line. About 35% of the comet's dust production is accounted for by the jets, about 20% is from the fan, and about 15% is in other fans. About 30% of the dust appears above the nightside hemisphere (*Boice et al.,* 2002). This may well be material emitted from the dayside hemisphere, appearing on the nightside due to projection effects. The comet's active area has been estimated at approximately 8% of the total surface (*Boice,* 2002).

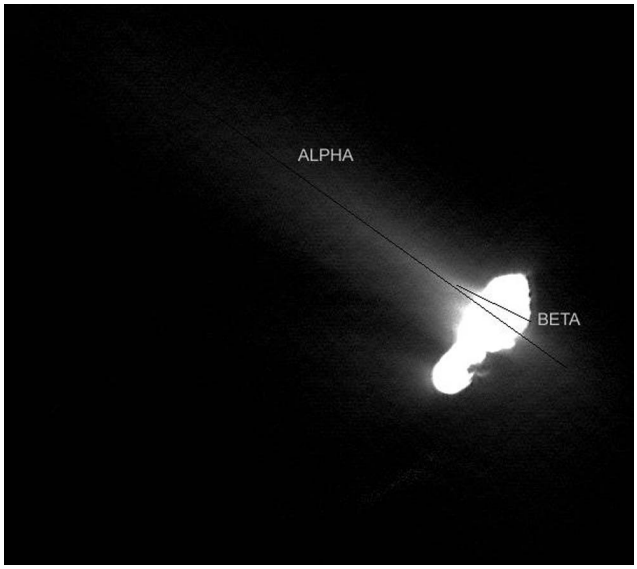

Fig. 8. The dominant dust emission on the sunward side is divided into α and β jets. The α jet is aligned at the core of the main jet. The β jet shown here is one of several roughly parallel smaller collimated jets. The range of this image is about 4825 km.

Hubble Space Telescope (HST) observations estimated the water production rate to $3.0 \pm 0.6 \times 10^{28}$ s^{-1} at the time of encounter, or about 600 kg s^{-1} (*Weaver et al.,* 2003). Integrated over Comet Borrelly's orbit the water mass loss per apparition would be approximately 2×10^{10} kg. Adding a similar amount of dust suggests an average erosion of the total surface between 0.5 and 1 m per apparition based on a density of the nucleus ≤1.000 kg m^{-3}. Water sublimation is strong enough to remove up to 10 m of surface layers at active areas (*Huebner et al.,*1986). For instance, the mesa slopes could retreat 10–20 m per apparition (*Britt et al.,* 2004). This level of erosion makes active cometary surfaces one of the most dynamic and rapidly changing features in the solar system.

4. COMPARISONS OF COMETS HALLEY, BORRELLY, AND ASTEROIDS

4.1. Comets Halley and Borrelly

The *Vega*, *Giotto*, and *DS1* measurements of cometary nuclei are far more similar than they are different. Both Comets Halley and Borrelly are irregularly shaped, very dark, and active over minor fractions of their surfaces (producing "jets"), and have surface temperatures close to those expected for a blackbody.

The nuclei show surface features inconsistent with a uniformly shrinking ellipsoid (or snowball) and some ten-

sile strength is apparent in protrusions such as the mountain or duck tail of Comet Halley or the canted low end of Comet Borrelly (see section 3.2). It is interesting that observations of structures have been interpreted by the *DS1* team using geological analogs — an approach not adopted by the *Giotto* team, for example. The stereo coverage resulting in a digital terrain model, better solar illumination, and less interference of the smaller dust production provide for a more detailed analysis of the surface features and morphology in the case of Comet Borrelly. Nonetheless, here too the similarities are more striking than the differences. The dark spots and ridges seen on Comet Borrelly (Fig. 7) are very similar to the chain of hills seen at Comet Halley (Fig. 3). The smooth terrain on Comet Borrelly is probably associated with activity and looks rather like the central depression on Comet Halley, which also shows evidence of activity (at least on its sunward extreme). The elevations on Comet Borrelly may be similar to the mountain feature on Comet Halley, while the mottled terrain is reminiscent of the region between the big active area and the chain of hills on Comet Halley.

Active regions appear to have slightly higher albedos than inactive regions, but nowhere does the albedo exceed 0.045 at the resolution of the images (around 50–100 m/pixel). It cannot be completely ruled out that there are small areas within these active regions that have (high) albedos closer to that of pure ice. The inhomogeneity of the surface activity and topography clearly influence the structure of the inner coma, making it difficult to extract information about the nature of the source, the initial acceleration, and particle fragmentation in the flow (*Ho et al., 2003*). While some preliminary conclusions on the structure of the source region may be possible, neither dataset is really good enough to distinguish between different surface emission models.

The similarities of both cometary nuclei are striking. There is no hint that comets originating from the Oort cloud (Comet Halley) look different from nuclei originating in the Edgeworth-Kuiper belt (Comet Borrelly) [see *Dones et al.* (2004) and *Duncan et al.* (2004) for discussions on these two cometary source regions].

The fortuitous observations of the complete outline of Comet Halley's nucleus, including its unilluminated parts, by HMC and the *Vega 1* and *2* images provide a reasonable shape model and the overall volume of the nucleus. This information is completely missing in the *DS1* data. It took three flybys to model the complex rotation of Comet Halley, even though the quality of the *Vega* images was not good enough to provide sufficient reference points for uncontroversial interpretations. No information on the rotation of Comet Borrelly can be expected from the *DS1* encounter.

4.2. Comet and Asteroid Surfaces

The images of Comets Halley and Borrelly highlight the similarities and differences between comets and other small bodies like asteroids and small moons. Photometric analysis of Comet Borrelly's nucleus suggests that it has a regolith and that its surface looks similar to that of asteroids. However, the processes at work on the two classes of bodies are very different. Comets Halley and Borrelly are characterized by a lack of impact craters and the existence of complex and sublimation-driven erosional features such as mesas, hills, and mottled terrain. Disk-resolved analysis of Comet Borrelly's roughness and particle phase function suggests that the comet does not get rougher with age, and that regions of the comet are infilled with or mantled by native dust. The surfaces of asteroids are dominated by impact craters. The energy to drive the asteroidal erosion process comes from episodic impact collisions, so this is necessarily a very slow process compared, e.g., to terrestrial erosive processes. Cometary erosion is driven by sublimation of volatiles during the cometary perihelion passage around the Sun. For Jupiter-family comets like Borrelly with frequent perihelion passages, sublimation-driven erosion alters landforms at rates that would be fast even by terrestrial standards. Fundamentally, surfaces of comets are dominated by sublimation while the surfaces of asteroids are dominated by impacts.

4.3. The Nucleus Paradigm

The spacecraft flybys revealed dark, evolved, solid cometary nuclei. The nonvolatile compounds outweigh the ice (*McDonnell et al.,* 1991), quite in contrast to what was considered before the Comet Halley flybys when an upper limit for the dust to gas ratio of 0.3 was used for the engineering model (*Divine,* 1981). Hence, their overall physical properties are better characterized by the nonvolatile component and not by (water) ice (*Keller,* 1987). The extremely low reflectivity argues for a surface of high porosity in accord with the low bulk density of the whole nucleus. The low tensile strength and porosity of the material is also reflected in the frequent fragmentation of the dust particles leaving the nucleus within the gas stream (*Thomas and Keller,* 1990).

The limited areas of activity can hardly be discerned from the generally inert surface, but they do seem to be slightly more reflective. An active region on a Jupiter-family comet with a perihelion distance near 1 AU will lose about 5–10 m depth of surface layer per revolution around the Sun (*Huebner et al.,* 1986). Consequently, the interior (material with volatiles that surfaces in active areas) looks similar to the material of the (inert) surface. The nucleus consists of a porous dust matrix that is in parts enriched with volatiles producing the activity. The inert surface layers are a crust of depleted matrix material that can form large topographic protrusions (the duck tail and mountain on Comet Halley and features such as mesas on Comet Borrelly). The fact that the surface temperature of the inert regions (comprising 80–90% of the surface area) reaches that of a blackbody is then unsurprising. In an active region, any loose mantle of dust (regolith) that might form would be blown away during perihelion passage (*Kührt and Keller,* 1994).

The present nuclei of Comets Halley and Borrelly are the small remnants of frequent splittings and shedding of blocks of material. Estimates of the mass in Halley's associated meteor streams show that its original mass 2000 to 3000 revolutions ago was 5–10 times bigger (*Hughes,* 1985).

The splitting is facilitated by the physical inhomogeneity of the nucleus agglomerated from subnuclei. The observed topography with typical scalelengths from 0.5 to 1 km (chain of hills, mottled terrain, dark spots) to the highly elongated shapes of the nuclei of Comets Halley and Borrelly, with indications of a "waist," reflects their inner structure.

The difficult detection and first characterization of the nucleus of Comet Halley in 1986 provided the fundamental data for our understanding of the nature of comets. It took 15 years to confirm these observations and to extend the conclusions to a second object.

Comet Halley is the most productive short-period comet, but yet only a minor fraction of its surface is active. Typical Jupiter-family comets display activity levels one or two magnitudes less than this, e.g., Comet Borrelly. How is activity at this low level maintained over many revolutions around the Sun? How does activity really work? The physical explanation of this phenomenon is a key to our understanding of comets. The answer will require new missions where the onset and details of activity can be studied in depth.

5. OUTLOOK

While Earth-based observations are now able to determine the sizes, approximate shapes, and possibly rotational characteristics of cometary nuclei (and hence may provide statistics), the next major step in the study of cometary nuclei will come from future space missions dedicated to their detailed investigation. The first of these will be NASA's Discovery mission, *Stardust*, which will provide information on the nonvolatile composition of the nucleus of Comet 81P/Wild 2. The physical structure of the particles, along with information on their strength, size, and shape, will provide us with some understanding of how structures on the nucleus can form and how the nucleus as a whole came together. The emphasis of this mission is on the sample return. Nevertheless, the navigation camera produced images of the nucleus of unprecedented quality, showing a rough surface with a large number of crater-like features (Fig. 9).

The *Deep Impact* mission will crash a block of copper into Comet 9P/Tempel 1 and study the effects of the impact. This will tell us about the tensile strength and porosity of the nucleus. The impact will also expose pristine material from the interior of the nucleus and we will be able to assess its chemical characteristics with a broad range of analytical instruments onboard the spacecraft. It is a testament to our lack of knowledge of the physical properties of cometary nuclei that many widely different scenarios for the impact are still being considered by the flight team as plausible.

Whatever the mission, the flybys of Comet Halley and of Comet Borrelly clearly show that for the interpretation of surface properties and physical characteristics of the nuclei, high-resolution imaging from different angles and at different phase angles is required. The quality of the information can be significantly improved with digital terrain models derived from stereoscopic views. The overall size and shape of a cometary nucleus as well as its rotation parameters can only be accessed by multiple flybys or, even better, by a comet rendezvous where the spacecraft orbits the nucleus.

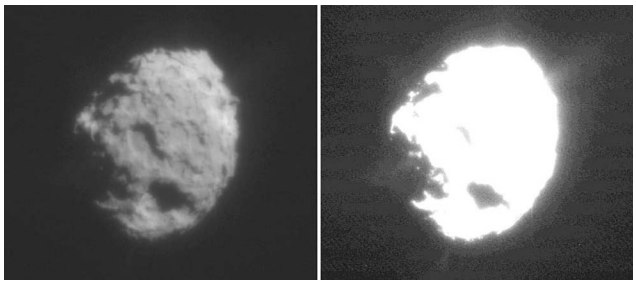

Fig. 9. The nucleus of Comet Wild 2 is shown in this image taken by the *Stardust* nagivation camera during the spacecraft's closest approach to the comet on January 2, 2004. The largest visible dimension is about 5 km. The image was taken within a distance of 500 km of the comet's nucleus. (The image was produced for distribution via the Web, and does not represent the final quality.) From the NASA *Stardust* Web page (Principal Investigator D. Brownlee, University of Washington, Seattle).

The European Space Agency's *Rosetta* mission is such a rendezvous mission. Originally, the *Rosetta* spacecraft was to be launched in January 2002 to meet with Comet 46P/Wirtanen at 3.5 AU from the Sun. Difficulties with the launcher required a new orientation of the mission. The second launch attempt was successful in March 2004. Its new goal is Comet 67P/Churyumov-Gerasimenko. The *Rosetta* spacecraft will deposit a science package on the surface of the nucleus and then continue to monitor the nucleus right through perihelion. If successful, this ambitious mission would study the nucleus surface down to a resolution of 2 cm/pixel from orbit and provide detailed measurements at even higher resolution from the lander. A strong complement of remote sensing (cameras, spectrometers, tomographic radio experiment) and *in situ* (ion and neutral mass spectrometers, dust analyzer, charge particle analyzer) instruments will observe the nucleus and its activity.

Activity could be monitored, compositional changes followed, surface temperatures tracked, and the internal structure assessed. It is the activity that characterizes comets and leads us to think of them as relics from the formation of the solar system. Hence, the emphasis *Rosetta* places on studying the nuclear activity should be highly rewarded.

In the distant future, the ultimate objective will be a sample return mission that can place strong constraints on the models of cometary origin and formation and, hence, on studies of the evolution of the solar system as a whole.

REFERENCES

Abergel A. and Bertaux J.-L. (1995) Calibration on the ground and in space. In *Images of the Nucleus of Comet Halley, Vol. 2* (R. Reinhard and B. Battrick, eds.), pp. 43–52. ESA SP-1127,

Noordwijk, The Netherlands.
Belton M. J. S. (1990) Rationalization of Halley's periods: Evidence for an inhomogeneous nucleus? *Icarus, 86,* 30–51.
Belton M. J. S., Julian W. H., Anderson A. J., and Mueller B. E. A. (1991) The spin state and homogeneity of Comet Halley's nucleus. *Icarus, 93*, 183–193.
Boice D. C., Britt D. T., Nelson R. M., Sandel B. R., Soderblom L. A., Thomas N., and Yelle R. V. (2002) The near-nucleus environment of 19/P Borrelly during the Deep Space One encounter (abstract). In *Lunar and Planetary Science XXXIII,* Abstract #1810. Lunar and Planetary Institute, Houston (CD-ROM).
Britt D. T, Buratti B. J., Boice D. C., Nelson R. M., Campins H., Thomas N., Soderblom L. A., and Oberst J. (2004) The morphology and surface processes of Comet 19P/Borrelly. *Icarus, 167,* 45–53.
Buratti B. J. and Mosher J. A. (1995) The dark side of Iapetus: Additional evidence for an exogenous origin. *Icarus, 115,* 219–227.
Buratti B. J., Hicks M. D., Oberst J., Soderblom L. A., Britt D. T., and Hillier J. K. (2004) Deep Space 1 photometry of the nucleus of Comet P/19 Borrelly. *Icarus, 167,* 16–29.
Crifo J. F. and Rodionov A. V. (1999) Modelling the circumnuclear coma of comets: Objectives, methods and recent results. *Planet. Space Sci., 47,* 797–826.
Crifo J. F., Rodionov A. V., Szegö K., and Fulle M. (2002) Challenging a paradigm: Do we need active and inactive areas to account for near-nuclear jet activity? *Earth Moon Planets, 90,* 227–238.
Divine N. (1981) Numerical models for Halley dust environments. In *The Comet Halley Dust & Gas Environment* (B. Battrick and E. Swallow, eds.), pp. 25–30. ESA SP-174, Noordwijk, The Netherlands.
Dones L., Weissman P. R., Levison H. F., and Duncan M. J. (2004) Oort cloud formation and dynamics. In *Comets II* (M. C. Festou et al., eds.), this volume. Univ. of Arizona, Tucson.
Duncan M., Levison H., and Dones L. (2004) Dynamical evolution of ecliptic comets. In *Comets II* (M. C. Festou et al., eds.), this volume. Univ. of Arizona, Tucson.
Emerich C. and 12 colleagues (1987a) Temperature of the nucleus of comet Halley. In *Symposium on the Diversity and Similarity of Comets* (E. J. Rolfe and B. Battrick, eds.), pp. 703–706. ESA SP-278, Noordwijk, The Netherlands.
Emerich C. and 11 colleagues (1987b) Temperature and size of the nucleus of comet P/Halley deduced from IKS infrared Vega-1 measurements. *Astron. Astrophys., 187,* 839–842.
Fernández Y. R., Jewitt C. D., and Sheppard S. S. (2001) Low albedos among extinct comet candidates. *Astrophys. J. Lett., 553,* L197–L200.
Hapke B. (1981) Bidirectional reflectance spectroscopy. I. Theory. *J. Geophys. Res., 86,* 3039–3054.
Hapke B. (1984) Bidirectional reflectance spectroscopy. 3. Correction for macroscopic roughness. *Icarus, 59,* 41–59.
Hapke B. (1986) Bidirectional reflectance spectroscopy. 4. The extinction coefficient and the opposition effect. *Icarus, 67,* 264–280.
Helfenstein P. and Veverka J. (1989) Physical characterization of asteroid surfaces from photometric analysis. In *Asteroids II* (R. Binzel et al., eds.), pp. 557–593. Univ. of Arizona, Tucson.
Hirao K. and Itoh T. (1987) The Sakigake/Suisei encounter with comet P/Halley. *Astron. Astrophys., 187,* 39–46.
Ho T.-M., Thomas N., Boice D. C., Köllein C., and Soderblom L. A. (2003) Comparative study of the dust emission of 19P/Borrelly (Deep Space 1) and 1P/Halley. *Adv. Space Res., 31(12),* 2583–2589.
Huebner W. F., Keller H. U., Wilhelm K., Whipple F. L., Delamere W. A., Reitsema H. J., and Schmidt H. U. (1986) Dust-gas interaction deduced from Halley Multicolour Camera observations. In *20th ESLAB Symposium on the Exploration of Halley's Comet, Vol. 2* (B. Battrick et al., eds.), pp. 363–364. ESA SP-250, Noordwijk, The Netherlands.
Huebner W. F., Boice D. C., Reitsema H. J., Delamere W. A., and Whipple F. L. (1988) A model for intensity profiles of dust jets near the nucleus of Comet Halley. *Icarus, 76,* 78–88.
Hughes D. W. (1985) The size, mass, mass loss and age of Halley's comet. *Mon. Not. R. Astron. Soc., 211,* 103–109.
Keller H. U. (1987) The nucleus of Comet Halley. In *Symposium on the Diversity and Similarity of Comets* (B. Battrick et al., eds.), pp. 447–454. ESA SP-278, Noordwijk, The Netherlands.
Keller H. U. (1989) Comets — Dirty snowballs or icy dirtballs? In *Proceedings of an International Workshop on Physics and Mechanics of Cometary Materials* (J. Hunt and T. D. Guyeme, eds.), pp. 39–45. ESA SP-302, Noordwijk, The Netherlands.
Keller H. U. and Jorda L. (2002) The morphology of cometary nuclei. In *The Century of Space Science* (J. A. M. Bleeker et al., eds.), pp. 1235–1275. Kluwer, Dordrecht.
Keller H. U. and 17 colleagues (1986) First Halley Multicolour Camera imaging results from Giotto. *Nature, 321,* 320–326.
Keller H. U., Kramm R., and Thomas N. (1988) Surface features on the nucleus of comet Halley. *Nature, 331,* 227–231.
Keller H. U., Markiewicz W. J., and Knollenberg J. (1992) Dust emission from cometary craters: Collimation of particle trajectories. *Bull. Am. Astron. Soc., 24(3),* 1018.
Keller H. U., Curdt W., Kramm J. R., and Thomas N. (1995) Images obtained by the Halley Multicolour Camera (HMC) on board the Giotto spacecraft. In *Images of the Nucleus of Comet Halley, Vol. 1* (R. Reinhard et al., eds.), pp. 1–252. ESA SP-1127, Noordwijk, The Netherlands.
Knollenberg J. (1994) Modellrechnungen zur Staubverteilung in der inneren Koma von Kometen unter spezieller Berücksichtigung der HMC-Daten der Giotto-mission. Ph.D. thesis, Georg-August-Universität, Göttingen, Germany.
Kührt E. and Keller H. U. (1994) The formation of cometary surface crusts. *Icarus, 109,* 121–132.
Kührt E., Knollenberg J., and Keller H. U. (1997) Physical risks of landing on a cometary nucleus. *Planet. Space Sci., 45,* 665–680.
Lamy P. L., Toth I., Grün E., Keller H. U., Sekanina Z., and West R. M. (1996) Observations of comet P/Faye 1991 XXI with the Planetary Camera of the Hubble Space Telescope. *Icarus, 119,* 370–384.
Lamy P. L., Toth I., and Weaver H. A. (1998) Hubble Space Telescope observations of the nucleus and inner coma of comet 19P/1904 Y2 (Borrelly). *Astron. Astrophys., 337,* 945–954.
Lamy P. L., Toth I., Fernández Y. R., and Weaver H. A. (2004) The sizes, shapes, albedos, and colors of cometary nuclei. In *Comets II* (M. C. Festou et al., eds.), this volume. Univ. of Arizona, Tucson.
Larson S., Sekanina Z., Levy D., Tapia S., and Senay M. (1987) Comet P/Halley near/nucleus phenomena in 1986. *Astron. Astrophys., 337,* 639–644.
Lyttleton R. A. (1953) *The Comets and Their Origin*. Cambridge Univ., Cambridge. 173 pp.
McDonnell J. A. M., Lamy P. L., and Pankiewicz G. S. (1991) Physical properties of cometary dust. In *Comets in the Post-Halley Era, Vol. 2* (R. L Newburn Jr. et al., eds.), pp. 1043–1073. Kluwer, Dordrecht.

Merényi E., Földy L., Szegö K., Toth I., and Kondor A. (1990) The landscape of comet Halley. *Icarus, 86,* 9–20.

Nelson R. M., Soderblom L. A., and Hapke B. W. (2004) Are the circular, dark features on Comet Borrelly's surface albedo variations or pits? *Icarus, 167,* 37–44.

Oberst J., Giese B., Howington-Kraus E., Kirk R., Soderblom L., Buratti B., Hicks M., Nelson R., and Britt D. (2004) The nucleus of Comet Borrelly: A study of morphology and surface brightness. *Icarus, 167,* 70–79.

Ockert M. E., Cuzzi J. N., Porco C. C., and Johnson T. V. (1987) Uranian ring photometry: Results from Voyager 2. *J. Geophys. Res., 92,* 14969–14978.

Peale S. J. (1989) On the density of Halley's comet. *Icarus, 82,* 36–50.

Rauer H., Hahn G., Harris A., Helbert J., Mottola S., and Oberst J. (1999) Nuclear parameters of comet P/Borrelly. *Bull. Am. Astron. Soc., 31,* 1131.

Rickmann H. (1989) The nucleus of comet Halley: Surface structure, mean density, gas and dust production. *Adv. Space Res., 9(3),* 59–71.

Rodionov A. V., Crifo J.-F., Szegö K., Lagerros J., and Fulle M. (2002) An advanced physical model of cometary activity. *Planet. Space Sci., 50,* 983–1024.

Sagdeev R. Z. (1988) Soviet space science. *Physics Today, 41(5),* 30–38.

Sagdeev R. Z., Avenesov G., Shamis V. A., Ziman Y. L., Krasikov V. A., Tarnopolsky V. A., Kuzmin A. A., Szegö K., Merényi E., and Smith B. A. (1986) TV experiment in Vega mission: Image processing technique and some results. In *20th ESLAB Symposium on the Exploration of Halley's Comet, Vol. 2* (B. Battrick et al., eds.), pp. 295–305. ESA SP-250, Noordwijk, The Netherlands.

Sagdeev R. Z., Elyasberg P. E., and Moroz V. I. (1988) Is the nucleus of comet Halley a low density body? *Nature, 331,* 240–242.

Sagdeev R. Z., Szegö K. Smith B. A., Larson S., Merényi E., Kondor A., and Toth I. (1989) The rotation of comet P/Halley. *Astron. J., 97,* 546–551.

Samarasinha N. H. and A'Hearn M. F. (1991) Observational and dynamical constraints on the rotation of Comet P/Halley. *Icarus, 93,* 194–225.

Schleicher D. G., Woodney L. M., and Millis R. L. (2003) Comet 19P/Borrelly at multiple apparitions: Seasonal variations in gas production and dust morphology. *Icarus, 162,* 415–442.

Schwarz G. and 11 colleagues (1986) Detailed analysis of a surface feature on Comet Halley. In *20th ESLAB Symposium on the Exploration of Halley's Comet, Vol. 2* (B. Battrick et al., eds.), pp. 371–374. ESA SP-250, Noordwijk, The Netherlands.

Soderblom L. A. and 21 colleagues (2002) Observations of Comet 19/P Borrelly by the Miniature Integrated Camera and Spectrometer aboard Deep Space 1. *Science, 296,* 1087–1091.

Stooke P. J. and Abergel A. (1991) Morphology of the nucleus of comet P/Halley. *Astron. Astrophys., 248,* 656–668.

Szegö K. (1995) Discussion of the scientific results derived from the near-nucleus images. In *Images of the Nucleus of Comet Halley, Vol. 2* (R. Reinhard and B. Battrick, eds.), pp. 68–80. ESA SP-1127, Noordwijk, The Netherlands.

Szegö K., Sagdeev F. L., Whipple A., Abergel J. L., Bertaux E., Merényi E., Szalaim S., and Varhalmi L. (1995) Images obtained by the Television System (TVS) on board the Vega spacecraft. In *Images of the Nucleus of Comet Halley, Vol. 2* (R. Reinhard and B. Battrick, eds.), pp. 1–255. ESA SP-1127, Noordwijk, The Netherlands.

Thomas N. and Keller H. U. (1987a) Comet Halley's near-nucleus jet activity. In *Symposium on the Diversity and Similarity of Comets* (E. J. Rolfe and B. Battrick, eds.), pp. 337–342. ESA SP-278, Noordwijk, The Netherlands.

Thomas N. and Keller H. U. (1987b) Fine dust structures in the emission of comet P/Halley observed by the Halley Multicolour Camera on board Giotto. *Astron. Astrophys., 187,* 843–846.

Thomas N. and Keller H. U. (1988) Global distribution of dust in the inner coma of comet P/Halley observed by the Halley Multicolor Camera. In *Dust in the Universe* (M. E. Bailey and D. A. Williams, eds.), pp. 540–541. Cambridge Univ., Cambridge.

Thomas N. and Keller H. U. (1989) The colour of comet P/Halley's nucleus and dust. *Astron. Astrophys., 213,* 487–494.

Thomas N. and Keller H. U. (1990) Interpretation of the inner coma observations of comet P/Halley by the Halley Multicolour Camera. *Ann. Geophys., 8,* 147–166.

Thomas N., Boice D. C., Huebner W. F., and Keller H. U. (1988) Intensity profiles of dust near extended sources on comet Halley. *Nature, 332,* 51–52.

Weaver H. A., Stern S. A., and Parker J. W. (2003) Hubble Space Telescope STIS observations of Comet 19P/Borrelly during the Deep Space 1 encounter. *Astron. J., 126,* 444–451.

Whipple F. L. (1950) A comet model I. The acceleration of Comet Encke. *Astrophys. J., 111,* 375–394.

Wilhelm K. (1987) Rotation and procession of comet Halley. *Nature, 327,* 27–30.